

**On the sub-band gap optical absorption in heat treated cadmium sulphide thin film deposited on glass by chemical bath deposition technique**

P. Chattopadhyay, B. Karim, and S. Guha Roy

Citation: *Journal of Applied Physics* **114**, 243506 (2013); doi: 10.1063/1.4853015

View online: <http://dx.doi.org/10.1063/1.4853015>

View Table of Contents: <http://scitation.aip.org/content/aip/journal/jap/114/24?ver=pdfcov>

Published by the [AIP Publishing](#)

---

**Articles you may be interested in**

[Chemical bath deposition of cadmium sulfide on graphene-coated flexible glass substrate](#)

*Appl. Phys. Lett.* **104**, 133902 (2014); 10.1063/1.4869850

[Fabrication and modification of chemical deposited nanocrystalline cadmium sulphide thin film in presence of impurity](#)

*AIP Conf. Proc.* **1482**, 617 (2012); 10.1063/1.4757545

[ZnO nano flowers formation by microwave assisted chemical bath deposition technique](#)

*AIP Conf. Proc.* **1451**, 157 (2012); 10.1063/1.4732399

[CdS nanofilms: Synthesis and the role of annealing on structural and optical properties](#)

*J. Appl. Phys.* **111**, 043519 (2012); 10.1063/1.3688042

[Direct evidence of Cd diffusion into Cu\(In,Ga\)Se 2 thin films during chemical-bath deposition process of CdS films](#)

*Appl. Phys. Lett.* **74**, 2444 (1999); 10.1063/1.123875

---



**Not all AFMs are created equal**  
**Asylum Research Cypher™ AFMs**  
**There's no other AFM like Cypher**

[www.AsylumResearch.com/NoOtherAFMLikeIt](http://www.AsylumResearch.com/NoOtherAFMLikeIt)

**OXFORD**  
INSTRUMENTS  
*The Business of Science®*

# On the sub-band gap optical absorption in heat treated cadmium sulphide thin film deposited on glass by chemical bath deposition technique

P. Chattopadhyay, B. Karim, and S. Guha Roy

*Department of Electronic Science, University of Calcutta, 92, A.P.C. Road, Kolkata 700009, India*

(Received 22 January 2013; accepted 6 December 2013; published online 26 December 2013)

The sub-band gap optical absorption in chemical bath deposited cadmium sulphide thin films annealed at different temperatures has been critically analyzed with special reference to Urbach relation. It has been found that the absorption co-efficient of the material in the sub-band gap region is nearly constant up to a certain critical value of the photon energy. However, as the photon energy exceeds the critical value, the absorption coefficient increases exponentially indicating the dominance of Urbach rule. The absorption coefficients in the constant absorption region and the Urbach region have been found to be sensitive to annealing temperature. A critical examination of the temperature dependence of the absorption coefficient indicates two different kinds of optical transitions to be operative in the sub-band gap region. After a careful analyses of SEM images, energy dispersive x-ray spectra, and the dc current-voltage characteristics, we conclude that the absorption spectra in the sub-band gap domain is possibly associated with optical transition processes involving deep levels and the grain boundary states of the material. © 2013 AIP Publishing LLC. [<http://dx.doi.org/10.1063/1.4853015>]

## I. INTRODUCTION

The measurement of optical properties of thin cadmium sulphide films<sup>1-4</sup> often exhibits an absorption tail when the photon energy is less than the band gap energy of the material. Such an absorption tail has been originally observed in the case of silver halides.<sup>5,6</sup> The results have been accounted for by an exponential rule near the absorption edge (widely referred to as Urbach rule), which has become a universal empirical law for wide range of materials. Extensive investigations in this area of optical absorption have resulted in different proposals with a view to explain the origin of Urbach tail. These proposals include description of absorption processes in terms of phonons and excitons,<sup>7</sup> thermal fluctuation of band gap energy,<sup>8</sup> and band tailing effect.<sup>9</sup> It is however well known that, apart from the above physical processes, the absorption spectra are sensitive to material processing conditions, such as substrate heating during material deposition or postdeposition annealing of the sample. The effect of substrate heating on the absorption co-efficient of CdS film has been reported by Pal *et al.*<sup>1</sup> The sensitivity of the optical properties of these materials to the annealing temperature has also been noticed.<sup>2-4</sup> Thus, the annealing temperature may have an additional impact on the sub-band gap optical absorption. Moreover, when the material is in polycrystalline form, there can be imperfections in the form of grain boundary states and potentials.<sup>10-12</sup> Such imperfections can also influence the sub-band gap optical absorption processes. Thus, the optical absorption in the sub-band gap region is still a matter of concern specifically when the materials are in polycrystalline forms. It would therefore be interesting to study the features of the absorption spectra of polycrystalline material in the light of Urbach rule, when the photon energy is less than the band gap energy of the materials. In order to study these issues more critically, we have considered a typical photosensitive material in the form of polycrystalline

cadmium sulphide and analyzed the absorption spectra of the material in the sub-band gap region under different annealing conditions. The results of such an investigation are reported in this communication.

## II. THREE-REGION DESCRIPTION OF OPTICAL ABSORPTION CURVES

In order to examine different processes involved in optical absorption in cadmium sulphide thin films, we split an absorption curve into three regions, namely, regions I, II, and III. The region I represents a domain of constant absorption described by an absorption coefficient nearly independent of photon energy. The region II corresponds to Urbach region where optical absorption can be effectively described by Urbach exponential rule. One may consider a general form for the Urbach exponential rule by following Kurik<sup>7</sup> and express the absorption tail as

$$\alpha = \alpha_0 \exp(h\nu/E_0). \quad (1)$$

In writing the Urbach rule in the above form, we have absorbed the constants in the general form of  $\alpha$  in Ref. 7 in the parameters  $\alpha_0$  and  $E_0$ . The term  $E_0$ , hereinafter referred to as Urbach energy, is an inverse of steepness of the absorption edge as described in Ref. 7. The region III represents a band-to-band transition region near the absorption edge may be described by the well known relation for the absorption coefficient given by  $\alpha = A (h\nu - E_g)^{1/2}$ , where  $A$  is a constant independent of energy and  $E_g$  is the band gap energy of the material. We have shown in Fig. 1, the representative absorption curves drawn for a given set of absorption parameters. To illustrate the role of absorption processes on the determination of the band gap of the material, we have generated in the inset, the familiar  $\alpha^2$  vs.  $h\nu$  plot by considering the Urbach rule and the values of the absorption coefficients

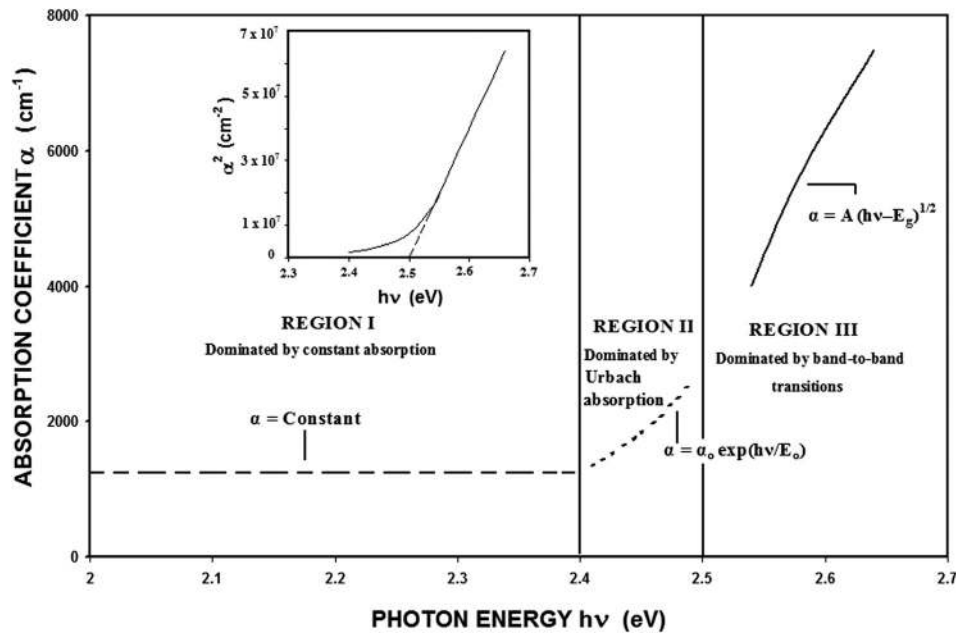


FIG. 1. Three-region representation of optical absorption curve of a semiconductor. The region I corresponds to a domain of photon energy where a constant absorption process dominates, may be described by a constant absorption coefficient (represented by a dashed line curve). As the energy exceeds a critical value, the Urbach absorption described by Urbach exponential rule (dotted line curve) dominates over the constant absorption process (Region II). The band-to-band transition (Region III) becomes important when photon energy exceeds the band gap energy. The variation of  $\alpha$  in this region is represented by a solid line curve. The inset shows a plot of  $\alpha^2$  vs.  $h\nu$  generated using the absorption coefficients of Urbach and band-to-band transition regions. As shown, the linear region of the curve when extrapolated to the  $h\nu$  axis (shown by broken line) yields the band gap energy. Parametric values used for calculations:  $\alpha_0 = 1.2 \times 10^{-5} \text{ cm}^{-1}$ ,  $E_0 = 0.13 \text{ eV}$ ,  $A = 2 \times 10^4 \text{ cm}^{-1} \text{ eV}^{-1/2}$ , and  $E_g = 2.5 \text{ eV}$ .

in the band-to-band transition region. It is seen that such a  $\alpha^2$  vs.  $h\nu$  plot is generally nonlinear. However, by using the linear region, one can determine the band gap of the material by the method of extrapolation (shown by broken line in the inset). The above scheme of segmentation of absorption curve into different regions has been adopted in the present work for analyzing critically the salient features of absorption spectra of cadmium sulphide thin films.

### III. MATERIAL DEPOSITION AND MEASUREMENTS

For the deposition of the CdS films, we have used the chemical bath deposition (CBD) technique.<sup>13–17</sup> The composition of the chemical bath reported in Ref. 13 has been used to deposit CdS films on glass substrate. Prior to the deposition of the films, the substrates are cleaned ultrasonically in distilled water, trichloroethylene, acetone and methanol and subsequently treated in a solution of  $\text{H}_2\text{O}_2$  and  $\text{H}_2\text{SO}_4$  prepared in 1:1 proportion and finally, cleaned in water and immersed in a chemical bath containing  $\text{CdCl}_2$ , ammonium acetate, thiourea and ammonium hydroxide. The temperature of the chemical bath has been maintained within  $65^\circ\text{C}$  to  $75^\circ\text{C}$ . The solution has been continuously stirred until the deposition of CdS film is completed. The thickness of the CdS film has been measured with a surface profilometer. The average value of the thickness of the film has been found to be  $0.88 \mu\text{m}$ .

The deposited CdS films have been given heat treatment at  $50^\circ\text{C}$ ,  $100^\circ\text{C}$ ,  $150^\circ\text{C}$ , and  $200^\circ\text{C}$  for 30 min in open air. The absorption spectra of the films have been measured with spectrophotometer in the wavelength range to 200 nm to 2600 nm. The surface morphology and composition of the

films have been examined by scanning electron microscope and energy dispersive x-ray analysis, respectively. For each of the samples, the dc current-voltage measurements are made by establishing indium contact on the samples by resistive evaporation. The data so measured are analyzed to extract the charge density at the grain boundaries.

### IV. RESULTS AND DISCUSSIONS

Fig. 2 shows the absorption spectra of as-deposited and heat treated samples. In the Urbach region, the percentage of optical transmission of light through the CdS samples has been found to vary under different annealing temperatures and varying photon energy. The % transmission varies from 1.74% to 3.78% for as-deposited CdS sample, 6.57%–17.08% for the sample annealed at  $50^\circ\text{C}$ , 13.57%–28.91% for the sample annealed at  $100^\circ\text{C}$ , 11.76%–29.21% for the sample annealed at  $150^\circ\text{C}$ , and 9.32%–33.11% for the sample annealed at  $200^\circ\text{C}$  in the Urbach region. The values of the absorption coefficient have been found to be in the range of  $10^4 \text{ cm}^{-1}$  in the Urbach region, which are in conformity with the results reported in a number of earlier works.<sup>4,18–21</sup>

The measured absorption coefficients are used to determine the band gap energy of the material by applying the relation  $\alpha^2 = A^2 (h\nu - E_g)$ , which corresponds to band-to-band transition region near the absorption edge. As already discussed in Sec. II that, although a plot of  $\alpha^2$  as a function of  $h\nu$  is generally nonlinear, the linear segment of such plot can be used for the determination of the band gap of the material. The above nature of nonlinear variation in the  $\alpha^2$  vs.  $h\nu$  plots for the as-deposited and annealed CdS samples is shown in Fig. 3. Such a nonlinearity arises because of the

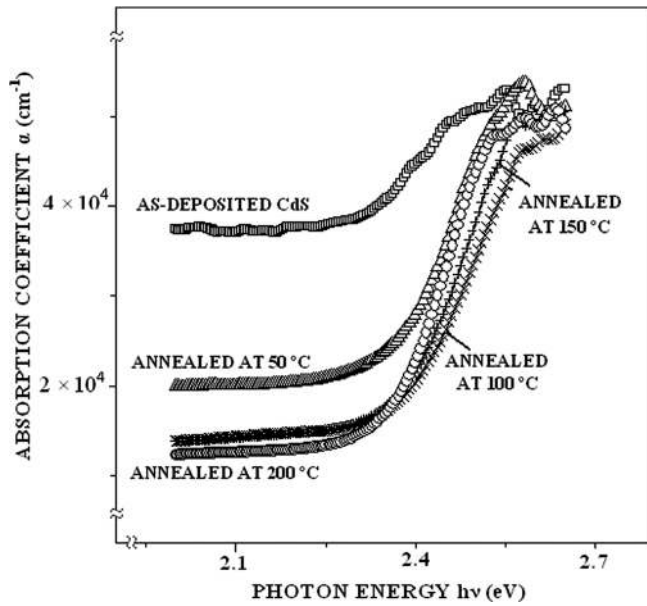


FIG. 2. The variation of the optical absorption co-efficient,  $\alpha$  for as-deposited and annealed CdS thin films as a function of photon energy  $h\nu$ .

dominance of respective absorption processes operative in the Urbach region and band-to-band transition region. The contribution from Urbach region however becomes less significant as the photon energy exceeds a certain critical value, which ultimately ensures band-to-band absorption process to dominate over Urbach absorption. This allows one to estimate the band gap of the material using the linear segment of the  $\alpha^2$  vs.  $h\nu$  curve as discussed in Sec. II. For the as-deposited sample, the absence of a clearly defined linear segment in the  $\alpha^2$  vs.  $h\nu$  curve constrained us to determine the band gap of the material. However, the linear regions of these plots for the annealed samples are found to be reasonably defined, which allowed us to determine the band gap of the material for different annealing temperatures. The band gap of the sample has been found to be 2.395 eV when

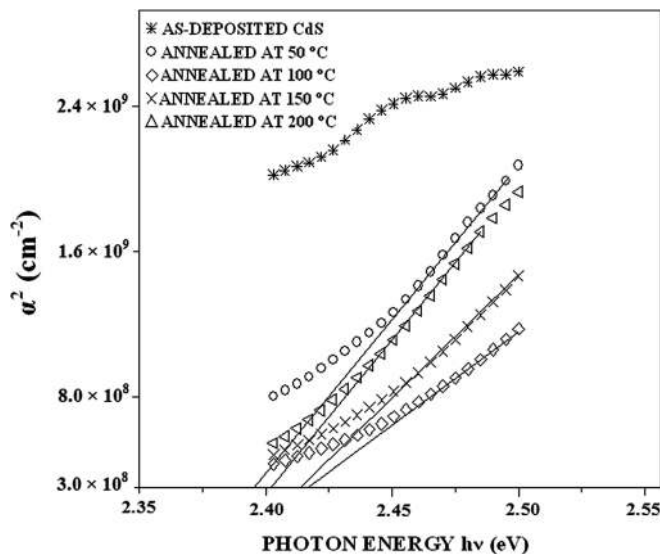


FIG. 3. The variation of the square of the optical absorption coefficient,  $\alpha^2$  as a function of photon energy  $h\nu$  for as-deposited and annealed CdS thin film.

annealed at 50 °C, which changes to only 2.413 eV when the annealing temperature has been increased to 200 °C. Similar change in the band gap of the material with annealing temperature has been reported by other workers. A change of band gap from 2.38 eV to 2.412 eV has been obtained by Pal *et al.*<sup>1</sup> when the CdS film is deposited at a substrate temperature of 200 °C. Roy and Srivastava<sup>17</sup> have found a change of band gap from 2.48 eV of the as-deposited sample to 2.45 eV after annealing at 200 °C. However, the change in band gap of the annealed samples with respect to as-deposited CdS sample remains inconclusive in the present case because of the uncertainty in fixing a linear region in  $\alpha^2$  vs.  $h\nu$  plot of the as-deposited sample.

For a particular annealing temperature, the absorption coefficient in region II of the absorption spectra has been found to vary exponentially with photon energy. However, it is found that the slope of the logarithmic variation of the absorption constant in this region does not correspond to  $1/kT$  as originally proposed by Urbach in the case of silver halides. Thus, Eq. (1) has been applied to extract the values of  $E_0$  and  $\alpha_0$  using the data in the Urbach region for as-deposited sample as well as for the samples annealed at temperatures 50 °C, 100 °C, 150 °C, and 200 °C. The variation of  $E_0$  with annealing temperature is shown in Fig. 4. It is seen that the estimated values of  $E_0$  can be fitted by an exponential relation given by

$$E_0(T_A) = E_0(0) \exp(-AT_A), \quad (2)$$

where  $E_0(0)$  and  $A$  are constants and  $T_A$  is the annealing temperature. The values of  $E_0(0)$  and  $A$  obtained by fitting the values of  $E_0(T_A)$  are found to be 3.012 eV and  $5.2 \times 10^{-3} \text{ K}^{-1}$ , respectively.

The above values of  $E_0$  have been used to determine the steepness parameter  $\sigma$  of the absorption curve ( $kT/E_0$ , in the present case). For as-deposited CdS film, the value of the

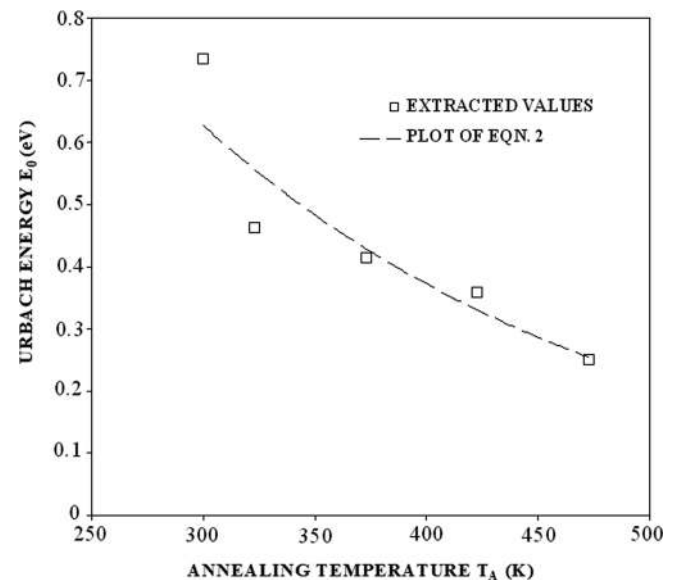


FIG. 4. The variation of Urbach energy,  $E_0$  as a function of annealing temperature,  $T_A$ . The values of  $E_0$  have been determined using Eq. (1) and the measured values of the optical absorption coefficient in region II of Fig. 2.

steepness parameter comes out to be 0.035. However, its value has been found to increase with annealing temperature. For the sample heated at 200 °C, the steepness parameter has been found to be 0.104. Such a dependence of steepness parameter on annealing temperature cannot be accounted for by applying models in Refs. 7 and 8 as these models apply to single crystals and that the process dependent physical changes (e.g., in the case of annealing) are not included in the model description. For instance, the steepness constant  $\sigma$  can be calculated by applying the relation<sup>7,8</sup>

$$\sigma = \sigma_0(2kT/\hbar\omega_p)\tanh(\hbar\omega_p/2kT), \quad (3)$$

where  $\hbar\omega_p$  is the phonon energy and the constant  $\sigma_0$  may depend upon electron-phonon interaction in the deformation potential approximation<sup>7</sup> or high temperature slope of the band-gap shift with temperature.<sup>8</sup> Now, considering the values of  $\sigma_0$  and  $\hbar\omega_p$  to be 2.17 and 7.5 meV, respectively,<sup>7</sup> the theoretical value of  $\sigma$  from Eq. (3) comes out to be 2.15 for CdS. The large discrepancy in the theoretical and experimental values of steepness constant can therefore be associated with polycrystalline nature of the sample used in our experiment.

The extraction procedure has also revealed a dependence of the pre-factor  $\alpha_0$  of the Urbach relation on annealing temperature. The logarithmic variation of  $\alpha_0$  as a function of annealing temperature is shown in Fig. 5. It is seen that the variation of  $\ln \alpha_0$  can be fitted by the relation

$$\ln \alpha_0 = -B_0 T_A + B_1, \quad (4)$$

where  $B_0 = 3.5 \times 10^{-2} \text{ K}^{-1}$  and  $B_1 = 17.24$ . In the same figure, we have plotted the experimental values of the absorption coefficient and cross-examined if the above empirical relations can regenerate the measured values of  $\alpha$ . It may be seen from the figure that Eq. (1) coupled with the relations given by Eqs. (2) and (3) describes the experimental variation of  $\alpha$  in region II. However, the variation of the

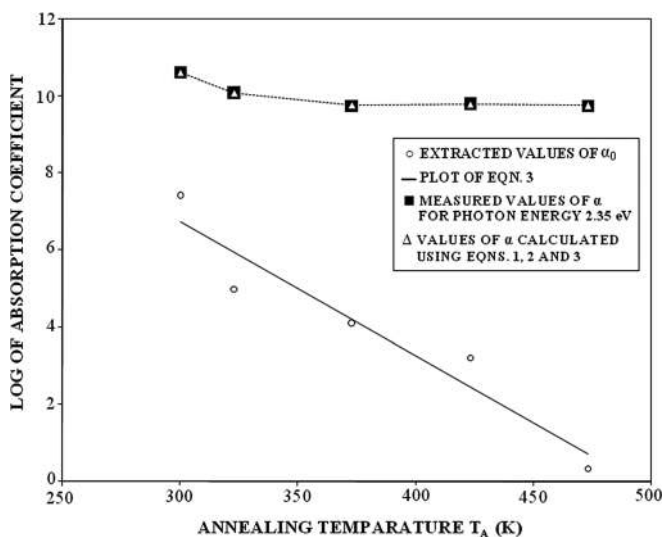


FIG. 5. The variation of the optical absorption co-efficient of CdS thin film in region II of Fig. 2 as a function of annealing temperature,  $T_A$  for photon energy,  $h\nu = 2.35 \text{ eV}$ .

absorption co-efficient described by Eq. (1) cannot account for the measured absorption coefficient in the region I. This is more evident from Fig. 6 where experimental values of the absorption co-efficient for the CdS sample heat treated at 200 °C are plotted as a function of photon energy and an attempt has been made to fit the absorption data with the help of Eq. (1). Clearly, Eq. (1) explains the absorption data up to certain energy in region II, but deviates considerably from the measured data at lower energies. The inadequacy of Urbach rule to describe absorption spectra below a certain photon energy hints towards two different transition processes in regions I and II, respectively. In particular, the optical absorption in region I is more like a constant absorption process in contrast to exponential Urbach rule. It is therefore apparent that the whole experimental absorption curve covering both the regions I and II cannot be explained on the basis of a single absorption process. The transition processes may be associated with defects of different kinds, such as grain boundary states<sup>10-12</sup> and deep levels.<sup>22-24</sup> The constant absorption processes at lower photon energies can be thought to be associated with deep centers in the individual grains having their energy levels comparable to the energies of the photons. This is further corroborated by the temperature dependence of the absorption curve in Fig. 2. It is seen that the absorption curve shifts downwards as a result of the heat treatment of the sample. Compared to the as-deposited sample, the shift is found to be large for sample annealed at  $T = 50 \text{ °C}$ , but gradually decreases at a much reduced rate for samples annealed at higher temperatures. We have plotted in Fig. 7, the values of the absorption coefficient in the constant region as a function of annealing temperature. It is found that the nature of variation of  $\alpha$  can be reasonably fitted by an empirical relation given by

$$\alpha = C_0 + C_1 \exp(-C_2 T_A), \quad (5)$$

where  $C_0 = 1.35 \times 10^4 \text{ cm}^{-1}$ ,  $C_1 = 4.12 \times 10^{11} \text{ cm}^{-1}$ , and  $C_2 = 5.5 \times 10^{-2} \text{ K}^{-1}$  are the fitting parameters. Though the absorption co-efficient  $\alpha$  varies nonlinearly with  $T_A$  according to Eq. (5), a logarithmic variation of  $\alpha - C_0$  as a function of  $T_A$  would be Arrhenius in nature. Since the absorption

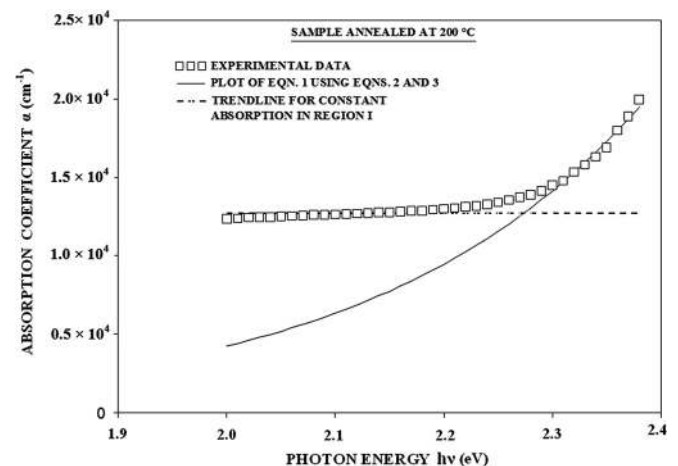


FIG. 6. The variation of the optical absorption coefficient,  $\alpha$  in regions I and II of the absorption spectra in Fig. 2 as a function of photon energy.

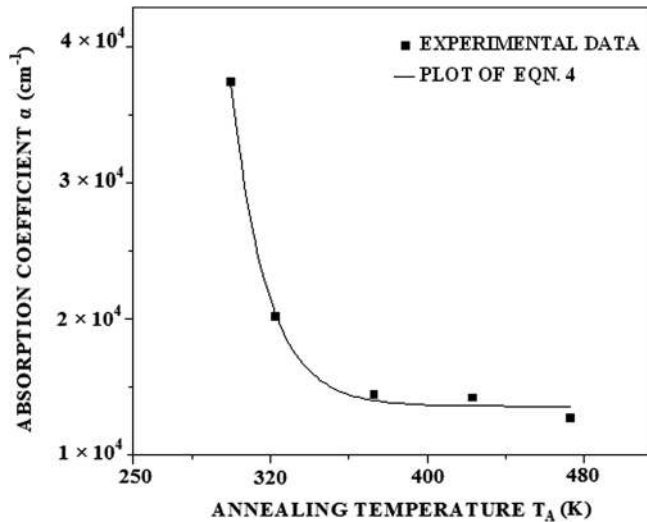


FIG. 7. The variation of optical absorption coefficient,  $\alpha$  in region I of Fig. 2 as a function of annealing temperature  $T_A$ .

processes at defect levels are likely to be controlled by the density of available and activated defects and defect energy, we apprehend co-relations of these quantities with  $\alpha$ - $C_0$ ,  $C_1$  and  $C_2$ , respectively.

A second kind of electronic transition may result due to distributed interface states at the grain boundaries. It may be mentioned here that the physical properties of grain boundaries and grain boundary interfaces have been extensively studied in the past and the density of grain boundary states may be in the range of  $10^{11}$ - $10^{13}$   $\text{cm}^{-2} \text{eV}^{-1}$ . For example, Pike and Seager<sup>10</sup> in their pioneering work considered a value of  $10^{16}$   $\text{m}^{-2} \text{eV}^{-1}$ , Yamamoto *et al.*<sup>25</sup> reported a distribution of density of states in the range  $\sim 10^{12}$ - $10^{14}$   $\text{cm}^{-2} \text{eV}^{-1}$  for polycrystalline silicon, Groot and Card<sup>26</sup> measured an energy distribution of interface states above  $10^{12}$   $\text{cm}^{-2} \text{eV}^{-1}$  at silicon grain boundaries, Madenach and Werner<sup>27</sup> reported energy distribution of interface states over the range  $\sim 10^{11}$ - $10^{12}$   $\text{cm}^{-2} \text{eV}^{-1}$  at silicon grain boundaries. In other polycrystalline semiconductors also, such as in InSb and CdTe, the density of grain boundary states have been found to be appreciable.<sup>28</sup> With the above values of the density of states, reported for different polycrystalline materials and a common experience of interface state density encountered in layered structures such as Schottky contacts,<sup>29,30</sup> this parameter cannot be ignored for the interpretation of physical properties of the material. In the present case of polycrystalline CdS, the density of grain boundary states has been reported to be quite large.<sup>31,32</sup> In fact, the density of grain boundary states plays a crucial role in fixing the grain boundary potential. The non-zero value of the grain boundary potential<sup>33-37</sup> and relatively high resistance of polycrystalline materials (compared to single crystals) conclusively prove manifestations of grain boundary states. It has been found that the grain boundary potential of CdS varies widely from sample to sample. This may be due to the fact that the grain boundary potential is sensitive to interface and bulk defect parameters.<sup>22</sup> A relation for grain boundary potential in the presence of donor-like deep levels and grain boundary states can be derived from Ref. 22 given by

$$\Psi_S = +(2\beta\delta + 1) - \left\{ (2\beta\delta + 1)^2 - 4\delta(\delta\beta^2 + \alpha\Psi_t) \right\}^{1/2}, \quad (6)$$

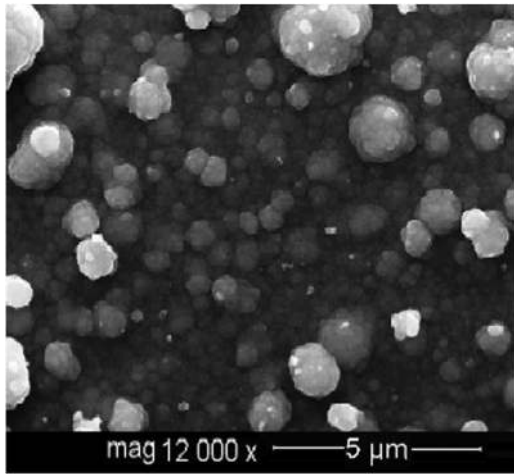
where

$$\alpha = N_t / (N_d + N_t),$$

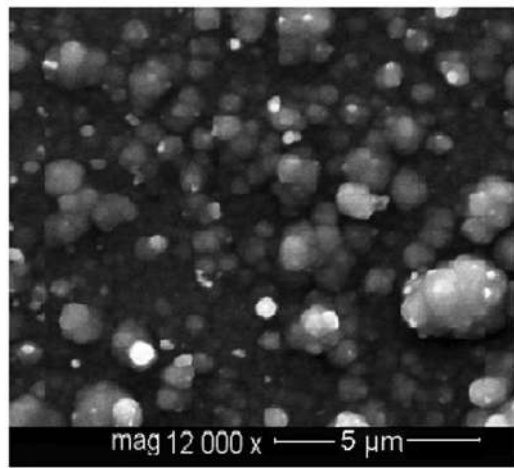
$$\beta = q^3 D_{it}^2 / 8\epsilon_s (N_d + N_t),$$

$$\delta = E_g - \phi_0 - V_n.$$

$N_t$  is the deep level density,  $N_d$  the doping concentration,  $D_{it}$  the density of grain boundary states,  $\phi_0$  the neutral level,  $\Psi_t$  the potential where the Fermi level intersects the deep level, and  $\epsilon_s$  is the permittivity of the material. With the values of interface state density in the range  $10^{11}$  to  $10^{13}$   $\text{cm}^{-2} \text{eV}^{-1}$ , doping concentration of the order  $10^{16}$   $\text{cm}^{-3}$ ,<sup>38</sup> deep trap density about  $10^{14}$   $\text{cm}^{-3}$ ,<sup>23</sup> and the neutral level to be 1.3 eV, we have estimated the grain boundary potential of polycrystalline CdS using the above relation. The calculated values of grain boundary potential are found to vary from 0.149 eV to 0.47 eV as the density of grain boundary states is varied from  $10^{11}$   $\text{cm}^{-2} \text{eV}^{-1}$  to  $10^{12}$   $\text{cm}^{-2} \text{eV}^{-1}$ . Thus, the variation in the experimental values of grain boundary potential can be attributed to different values of density of states possibly resulting from different processing conditions. Now, considering the above important effects of interface states influencing the material properties of polycrystalline materials, we propose the sharp change in the absorption co-efficient in the sub-band gap region is associated with the change in the interface state density due to annealing. Furthermore, an energy dependence of the density of grain boundary states<sup>10,25-27</sup> may yield an absorption tail which can be different from the absorption processes at the deep centers. The electronic transitions in such cases take place at the interface region of the two grains, which may also depend upon the modification of the grain boundary interfaces by different processing conditions, such as annealing at different temperature being investigated in the present work. To look for a possible explanation for the above effect of annealing, we closely examine the SEM images and EDS data of the samples shown in Figs. 8 and 9, respectively. It is found that the local density of grains increases upon annealing which may be a result of reorganization of the film.<sup>19</sup> This leads to a proximity effect resulting from a more compact/ordered arrangement of grains. The EDS results, however, suggest insignificant changes in the atomic percentage of cadmium, sulphur, and oxygen upon heat treatment, thereby indicating film composition to remain almost unaltered. Accordingly, it is unlikely that such a minor change in the composition could be a possible reason for the observed dependence of absorption coefficient on annealing temperature. However, the proximity effect as observed in SEM images can improve the grain boundary interface either due to shrinking of interface width or modification of grain boundary states or a combination of the both. An improvement of the grain boundary interface is also possible due to atomic migration which passivates the grain boundary states. All these possibilities may lead to a decrease in the grain boundary states leading to a lesser number of electronic transitions, which eventually results in



(A)

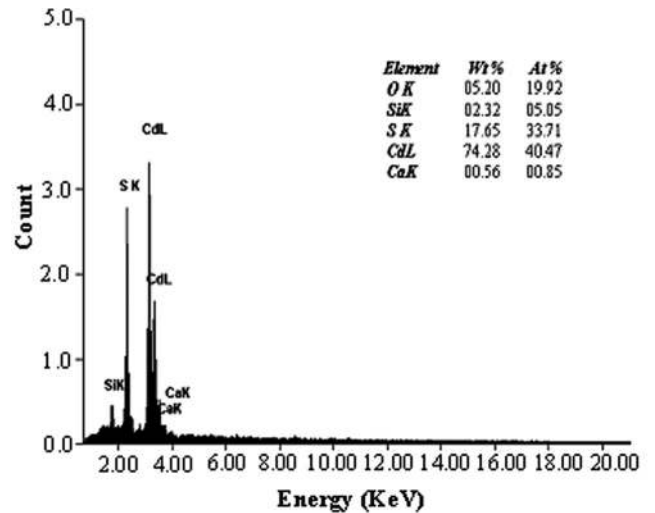


(B)

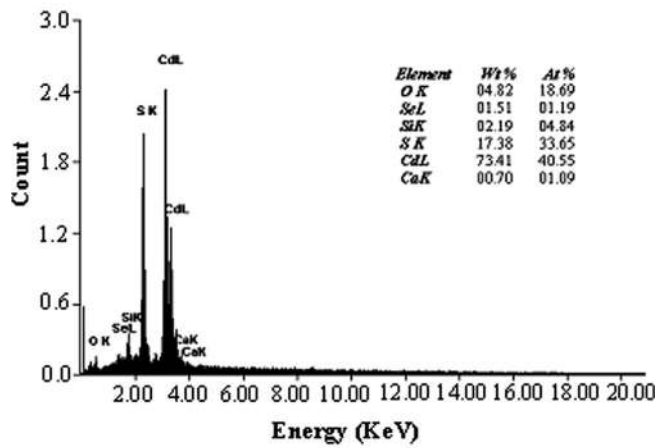
FIG. 8. The SEM images of CdS thin films: (A) as-deposited and (B) air-annealed at 200°C.

a decrease in the absorption coefficient of the material. Such a feature is reflected in the absorption curve, which shows decrease in the absorption coefficient upon heat treatment for a given value of photon energy in the Urbach region. It is well known that the grain boundary states in polycrystalline semiconductor are primarily responsible for free carrier trapping and the formation of grain boundary potential as a consequence of charge exchange with the adjacent grains in accordance with the charge neutrality condition of the system.<sup>10–12,22</sup> We therefore associate the above grain boundary states to be the main issue for the optical absorption in the Urbach region of the absorption spectra. The shift of absorption curve upon heat treatment may be linked with the reduction in the grain boundary interface states due to the close proximity of grains consistent with the surface morphology as seen from the SEM images.

A similar conclusion has been drawn on the basis of measured current-voltage characteristics of the samples at different annealing temperatures (Fig. 10). It is well known that, for a polycrystalline semiconductor, the carrier mobility decreases exponentially with the grain boundary potential.<sup>38,39</sup> In such cases, the I–V relation can be written as



(A)



(B)

FIG. 9. The EDS spectra of CdS thin films: (A) as-deposited and (B) air-annealed at 200°C.

$$I = qA_c N_d \mu_o \exp(-q\Psi_s/kT) V/L, \tag{7}$$

where  $\mu_o$  is the electron mobility corresponds to single crystal,  $A_c$  the area of contact,  $L$  the length between the contacts, and  $V$  is the applied voltage. The material resistance,  $R$ , can be obtained directly from the above relation given by

$$R = R_0 \exp(q\Psi_s/kT), \tag{8}$$

where  $R_0 = L/(qA_c N_d \mu_o)$  is the material resistance corresponding to a single crystal. The above equation therefore suggests an increase in the resistance when the material is in polycrystalline form. Now, by applying the charge neutrality condition given by  $Q_{sc} = Q_{it}$ , where  $Q_{it}$  is the grain boundary charge density and  $Q_{sc} = (2q\epsilon_s N_d \Psi_s)^{1/2}$ , the semiconductor depletion layer charge density, we obtain an expression for the resistance of a polycrystalline material in terms of grain boundary charge density given by

$$R = R_0 \exp\{Q_{it}^2 / (2kT\epsilon_s N_d)\}. \tag{9}$$

Thus, the interface state charge density at the grain boundary can be measured by applying the above equation in the following form:

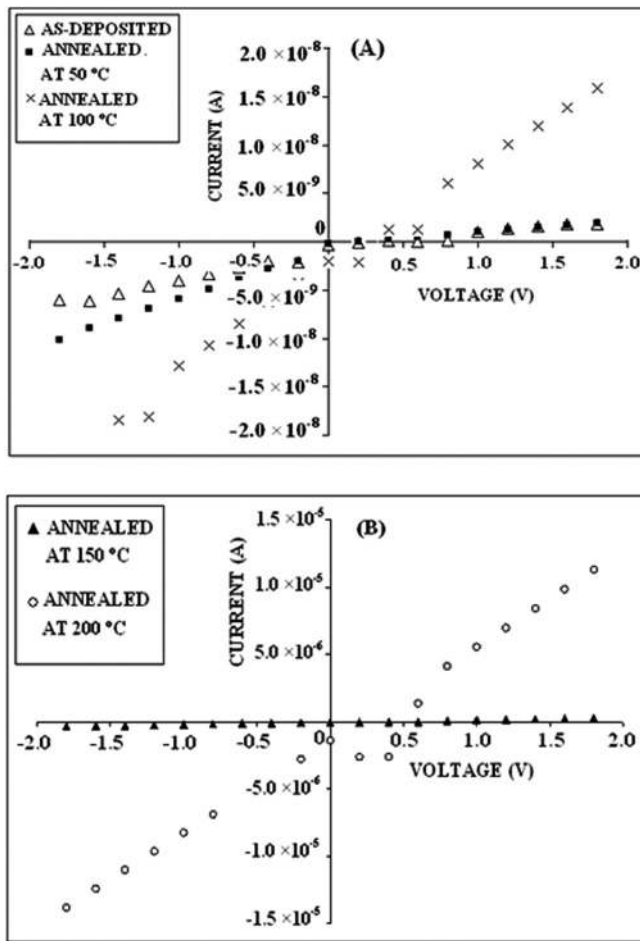


FIG. 10. The current-voltage characteristics of CdS thin films: (A) as deposited, and annealed at 50 °C and 100 °C, respectively; and (B) annealed at 150 °C and 200 °C, respectively.

$$Q_{it} = \{2kT\epsilon_s N_d \ln(R/R_0)\}^{1/2}. \quad (10)$$

To determine  $Q_{it}$  for the CdS samples, we have used the measured current-voltage data shown in Fig. 10. The current-voltage characteristics are found to be reasonably linear for the samples annealed at 100 °C, 150 °C, and

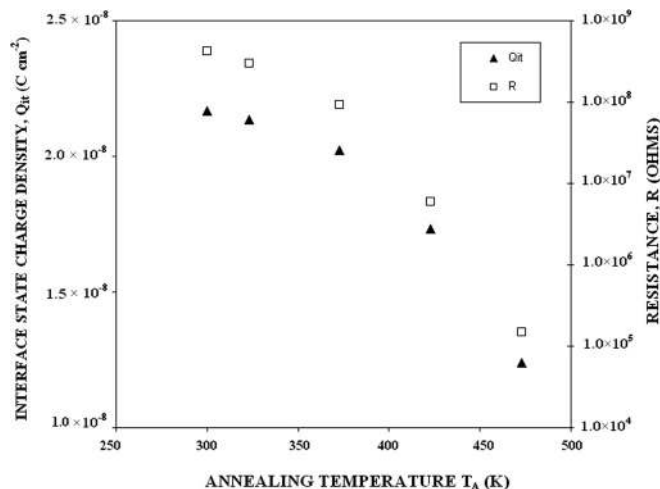


FIG. 11. The variation of resistance and interface state charge density at the grain boundaries of CdS samples as a function of annealing temperature.

200 °C, except for some scattering and asymmetry in transport observed for as-deposited sample and the sample annealed at 50 °C. Now, by fitting these characteristics linearly, the resistances of the samples are determined. Using the values of  $R_0 = 3.13 \times 10^3$  ohm and  $N_d = 10^{16}$   $cm^{-3}$ , we have estimated the values of  $Q_{it}$ . The variations of R and  $Q_{it}$  are shown in Fig. 11 as a function of annealing temperature. The decrease in the interface charge density  $Q_{it}$  with annealing temperature further confirms a decrease in the density of grain boundary states.

## V. CONCLUSIONS

In conclusion, the analyses of optical absorption curves of heat treated CdS films reveal the Urbach relation for sub-band gap absorption to be limited up to certain energy of the incident photons, below which the absorption coefficient becomes almost constant. Accordingly, a single optical transition process is inadequate to account for the measured absorption data in the sub-band gap energy domain. It is found that both the constant and Urbach regions of the absorption curve are functions of annealing temperature though the mechanisms of absorption appeared to be different for these two regions. While the constant absorption region can possibly be a result of optical transitions from deep levels, the absorption data in the Urbach region indicate grain boundary states to be the origin for causing optical transitions. An examination of SEM images in association with EDS results of the annealed samples strongly suggests a change in the grain size, thereby implying a more compact grain distribution leading to modification of grain boundary states and the grain boundary potential barriers. The analyses of the current-voltage characteristics of the samples reveal a reduction in the interface state charge density at the grain boundaries upon annealing, which further confirm interface states to be the reason for variation of the absorption coefficient in the Urbach region upon annealing of CdS samples at different temperatures.

<sup>1</sup>U. Pal, R. Silva-Gonzalez, G. Martinez-Montes, M. Gracia-Jimenez, M. A. Vaidal, and Sh. Torres, *Thin Solid Films* **305**, 345 (1997).

<sup>2</sup>J. Hiie, T. Dedova, V. Valdna, and K. Muska, *Thin Solid Films* **511–512**, 443 (2006).

<sup>3</sup>J. Barman, K. C. Sarma, M. Sarma, and K. Sarma, *Indian J. Pure Appl. Phys.* **46**, 339 (2008).

<sup>4</sup>A. J. Haider, A. M. Mousa, and M. H. Al-Jawad, *J. Semicond. Technol. Sci.* **8**, 326 (2008).

<sup>5</sup>F. Urbach, *Phys. Rev.* **92**, 1324 (1953).

<sup>6</sup>F. Moser and F. Urbach, *Phys. Rev.* **102**, 1519 (1956).

<sup>7</sup>M. V. Kurik, *Phys. Status Solidi A* **8**, 9 (1971).

<sup>8</sup>T. Skettrup, *Phys. Rev. B* **18**, 2622 (1978).

<sup>9</sup>S. John, C. Soukoulis, M. H. Cohen, and E. N. Economou, *Phys. Rev. Lett.* **57**, 1777 (1986).

<sup>10</sup>G. E. Pike and C. H. Seager, *J. Appl. Phys.* **50**, 3414 (1979).

<sup>11</sup>P. Chattopadhyay, *J. Phys. Chem. Solids* **56**, 189 (1995).

<sup>12</sup>P. Chattopadhyay, *Semicond. Sci. Technol.* **10**, 1099 (1995).

<sup>13</sup>M. Ray and P. Chattopadhyay, *Indian J. Pure Appl. Phys.* **35**, 349 (1997).

<sup>14</sup>H. El Maliki, J. C. Bernede, S. Marsillac, J. Pinel, X. Castel, and J. Pouzet, *Appl. Surf. Sci.* **205**, 65 (2003).

<sup>15</sup>A. Cortes, H. Gomez, R. E. Marotti, G. Riveros, and E. A. Dalchiele, *Sol. Energy Mater. Sol. Cells* **82**, 21 (2004).

<sup>16</sup>L. Wenyi, C. Xun, C. Qiulong, and Z. Zhibin, *Mater. Lett.* **59**, 1 (2005).

<sup>17</sup>P. Roy and S. K. Srivastava, *Mater. Chem. Phys.* **95**, 235 (2006).

<sup>18</sup>H. Metin and R. Esen, *J. Cryst. Growth* **258**, 141 (2003).

- <sup>19</sup>H. Metin and R. Esen, *Semicond. Sci. Technol.* **18**, 647 (2003).
- <sup>20</sup>B. R. Sankapal, R. S. Mane, and C. D. Lokhande, *Mater. Res. Bull.* **35**, 177 (2000).
- <sup>21</sup>Z. Rizwan, A. Zakaria, M. S. Mohd Ghazali, A. Jafari, F. U. Din, and R. Zamiri, *Int. J. Mol. Sci.* **12**, 1293 (2011).
- <sup>22</sup>P. Chattopadhyay, D. P. Haldar, S. Chakraborty, and M. Ray, *Phys. Status Solidi A* **142**, 117 (1994).
- <sup>23</sup>P. Besomi and B. Wessels, *J. Appl. Phys.* **51**, 4305 (1980).
- <sup>24</sup>M. Hussein, G. Lleti, G. Sagnes, G. Bastide, and M. Rouzeyre, *J. Appl. Phys.* **52**, 261 (1981).
- <sup>25</sup>I. Yamamoto, H. Kuwano, and Y. Saito, *J. Appl. Phys.* **71**, 3350 (1992).
- <sup>26</sup>A. W. De Groot and H. C. Card, *IEEE Trans. Electron Devices* **31**, 1370 (1984).
- <sup>27</sup>A. J. Madenach and J. H. Werner, *Phys. Rev. B* **38**, 13150 (1988).
- <sup>28</sup>R. P. Sharma, A. K. Shukla, A. K. Kapoor, R. Srivastava, and P. C. Mathur, *J. Appl. Phys.* **57**, 2026 (1985).
- <sup>29</sup>P. Chattopadhyay and A. N. Daw, *Solid-State Electron.* **29**, 555 (1986).
- <sup>30</sup>P. Chattopadhyay and B. Roychoudhuri, *Solid-State Electron.* **36**, 605 (1993).
- <sup>31</sup>E. Bertran, J. L. Morenza, and J. Esteve, *Thin Solid Films* **123**, 297 (1985).
- <sup>32</sup>H. Oumous and H. Hadiri, *Thin Solid Films* **386**, 87 (2001).
- <sup>33</sup>A. E. Rakhshani, *J. Phys.: Condens. Matter* **12**, 4391 (2000).
- <sup>34</sup>J. I. B. Wilson and J. Woods, *J. Phys. Chem. Solids* **34**, 171 (1973).
- <sup>35</sup>R. G. Mankarious, *Solid-State Electron.* **7**, 702 (1964).
- <sup>36</sup>C. A. Neugebauer, *J. Appl. Phys.* **39**, 3177 (1968).
- <sup>37</sup>C. Wu and R. H. Bube, *J. Appl. Phys.* **45**, 648 (1974).
- <sup>38</sup>R. H. Bube, *J. Chem. Phys.* **23**, 18 (1955).
- <sup>39</sup>R. L. Petritz, *Phys. Rev.* **104**, 1508 (1956).